Title
MAGNETIZATION AND A SUPER CONDUCTING SOLENOID

Author
Aron, Paul R.

Publication Date
1963-06-05

UCRL-10854

University of California

Ernest O. Lawrence Radiation Laboratory

MAGNETIZATION AND A SUPERCONDUCTING SOLENOID

To be submitted to Rev. Sci. Instr.

UCRL-10854

UNIVERSITY OF CALIFORNIA

Lawrence Radiation Laboratory
Berkeley, California

Contract No. W-7405-eng-48

MAGNETIZATION AND A SUPERCONDUCTING SOLENOID

Paul R. Aron

June 5, 1963

Magnetization and a Superconducting Solenoid

Paul R. Aron

Lawrence Radiation Laboratory
University of California
Berkeley, California

June 5, 1963

ABSTRACT

The relationship of the magnetization of Nb-25% Zr superconducting alloy and the magnetic field of a solenoid constructed of this material is discussed. Measurements of the magnetic field as a function of current, induced magnetic moment, history-dependent remnant moment, and other related properties are described. An approximate method of computing the magnitudes of these effects is discussed and the results are shown to agree with measurements. The coil critical current I_c is related to the short sample I_c, and the discrepancy is discussed in terms of the magnetization of Nb-Zr.

Magnetization and a Superconducting Solenoid*

Paul R. Aron†

Lawrence Radiation Laboratory
University of California
Berkeley, California

June 5, 1963

INTRODUCTION

In 1961 Kunzler[1] and others[2] demonstrated the existence of superconducting materials with high critical fields associated with high transport currents. Since that time there has been a concerted effort to construct magnets with volumes and fields appropriate for research in physics. Published and unpublished reports indicate that a large measure of success has been achieved. Magnets with fields as high as 68 kG over a diameter of 1/2 in. have been reported.[3] Magnets of lower fields (40 to 50 kG) but of larger diameter (2.5 to 5 in.) have also been described.[4,5] It would seem appropriate, then, to ask detailed questions as to the nature of the field in the magnet. For example: how does it depend on the current, or what is the spatial distribution of the field in the bore of the magnet? This investigation was undertaken in an attempt to reveal the magnitude of the deviations of the magnetic field from classical behavior. The deviations to be discussed result from the nature of the magnetization of the superconductor.

Figure 1 shows typical behavior in the M-H plane of a long cylindrical sample of Class-II superconducting heavily cold-worked alloy, Nb-25% Zr in a magnetic field parallel to its axis. Several features should be noted. First, there is the region of apparent perfect diamagnetic behavior,[6] which extends to 470 G, where flux begins to enter. Then the magnetization follows a roughly parabolic curve until at about 8 kG a flux jump occurs. This is a discontinuity in the magnetization curve that is associated with the evolution of heat,[7] presumably as the result of eddy-current losses in the normal regions of what must be a kind of intermediate-state structure. Then the behavior is repeated with varying deviation from the $\mu = 1$ line until a field near the resistive critical field is reached and the material exhibits normal-state behavior. Reduction of the applied field causes the curve to trace a similar kind of path which, though qualitatively a mirror image of the first curve, fails to show discontinuities at the same points. A remnant field is evident at H = 0. Repeated cycling of the M-H loop shows further complication of the behavior. The magnetization curve shown was taken on an 8.9-cm-long sample, 0.54 cm in diameter.

The wire in the winding of a magnet, however, is in a magnetic environment that is not as well understood and, therefore, only the general features of the curve shown are relevant to this discussion.

The theory of such magnetization curves is in a poor state at present. The most successful theory, due to Abrikosov,[8] can deal only with reversible phenomena. The work of Anderson[9] and of Kim[7] is relevant, but of little quantitative help, because a detailed understanding of the nature of the defect structure is required for useful predictions.

MAGNET

For the purposes of this investigation a small air-core solenoid was constructed of approximately 1 lb of Nb-25% Zr alloy wire, and its properties were studied at 4.2° K. The magnet had a critical current of 16.7 A, and a magnetic field of 41.5 kG on the axis. The bore was 1.28 cm in diameter and 3.63 cm long. The magnetic field was measured with a 0.5-cm-diam coil of No. 50 formvar insulated copper wire with an area-turns product of 593.4 cm^2. This coil was connected to a wide-band integrator circuit. (See Fig. 2 for details). The probe coil was wound in a modified flux-ball geometry such that it measures the field at its center rather than taking an average over its diameter.[10] It was further arranged that the probe could be moved along the axis of the magnet. For the measurements of H(z), the probe position was read out as a voltage which drove the y axis of an x-y plotter while the output of the integrator drove the x axis. In this way the axial distribution of the magnetic field was obtained. The magnet construction details are given below:

Length of coil	3.63 cm
Outside diameter	5.89 cm
Inside diameter	1.28 cm
Number of turns	9994
Length of wire	1120 m
Diameter of wire	0.0254 cm
Insulation (epoxy) thickness	0.0013 cm
Packing fraction	0.602
Coil form	Micarta
Wire supplier	Westinghouse
Winding technique	Layer wound with Mylar tape (0.0025 cm) between layers
Contacts	Wire ultrasonically tinned with a 50-50 Bi-Cd mixture soft-soldered over 7-cm length to copper block.

The magnetic field on the axis of a superconducting solenoid, $H(z)$, can be expressed as the sum of an applied magnetic field $H_a(z)$ and a magnetic field $H_m(z)$ due to the magnetization of the superconductor, $\underset{\sim}{M}$:

$$H(z) = H_a(z) + H_m(z). \qquad (1)$$

Here H_m is the sum of the remnant magnetization field H_r, and the induced magnetization field H_I. Following Montgomery,[11] and writing $H(z)_i$ as the axial field due to a ring of magnetic material characterized by a magnetization M, assumed constant over the volume Δv_i, we have

$$\Delta H_m(z)_i = M_i \int_{\Delta v_i} \frac{(3\cos^2\phi - 1)\cos\theta_i - 3\sin\phi\cos\phi\sin\theta_i}{r^3}\,dv\,, \qquad (2)$$

where θ_i is the angle between M_i and z, r is the magnitude of the radius vector to the point of interest z, and ϕ is the angle between $\underset{\sim}{r}$ and the z axis, as indicated in Fig. 3. A solenoid, owing to the variation of the magnetic field over the volume of its windings, is not expected to exhibit a constant M over its volume in the self-excited case. Use of the subscript i permits one to consider the coil as subdivided into a number of regions Δv_i over which M_i can be taken as constant Then we have

$$H_m(z) = \sum_i^m \Delta H_m(z)_i\,. \qquad (3)$$

The accurate prediction of the history dependence and current dependence of H(z) then becomes a matter of knowing M_i as a function of history and magnetic field, knowing what is meant by $H_a(z)$, and performing the appropriate summation. Figure 1 implies that the behavior of the quantity M_i is not simple nor necessarily reproducible. Further, it is not clear in all cases what to take as $H_a(z)$. It will be assumed, however, in the analyses of the experimental data that $H_a(z)$ is either the applied magnetic field or, in the self-excited case, the field that would appear in the magnet for $M_i \equiv 0$. The quantity $H_m(z)$ can be thought of as the deviation from what will be called $\mu = 1$ or classical behavior.

Applied Magnetic Field Case

To determine the effective magnetization of the Nb-Zr alloy in the coil configuration, the magnet was placed in a uniform magnetic field oriented parallel to the magnet axis. The average magnetization $M(H_a)$ could then be obtained by measurement of H(z) and the application of Eq. (2), which in this simple case can be reduced to

$$H_m(z) = -2\pi M\left[\frac{1}{(\alpha_1+1)^{1/2}} - \frac{1}{(\alpha_2+1)^{1/2}} + \frac{1}{(\beta_1+1)^{1/2}} - \frac{1}{(\beta_2+1)^{1/2}}\right]. \qquad (4)$$

Here $\alpha_1 = \left(\frac{r_1}{\ell - z}\right)^2$, $\beta_1 = \left(\frac{r_1}{\ell + z}\right)^2$,

$\alpha_2 = \left(\frac{r_2}{\ell - z}\right)^2$, $\beta_2 = \left(\frac{r_2}{\ell + z}\right)^2$,

r_1 = inner radius,

r_2 = outer radius,

2ℓ = total length of coil,

z = axial coordinate as measured from the center of the coil.

The history dependence of the remnant magnetization M_r, and the induced magnetization M_I, was determined by the following procedure:

1. Cool coil to 4.2° K in zero field,
2. Raise H_a to first point,
3. Measure H(z),
4. Reduce H_a to zero,
5. Measure H(z),
6. Raise H_a to next higher point and continue repeating sequence 2 to 6 until the highest field (80 kG) is achieved.

The dependence of $-4\pi M_I$ on H_a as determined from step 3 is given in Fig. 4. The bars indicate the probable error, which is seen to increase strongly at higher fields. This increase is due to the poor regulation of the magnet power supply and to the increasing difficulties with nonuniformity of H_a over the length of the coil. The results, however, seem adequate to indicate the general nature of the magnetization curve.

The initial slope corresponds to nearly complete exclusion of flux from the winding volume. This is somewhat surprising, since the ratio of superconductor volume to winding volume (λ) is 0.602, and it is certain that the measurement would detect flux corresponding to this value of λ. The experimental data indicate that the appropriate value of λ is more nearly 1. This must be due to the shielding of a wire by the wires above and below so that flux can thread the coil only parallel to the axis between the layers. The ratio between the layer-to-layer distance and the diameter of the superconductor is 0.90, a more appropriate value. There is a deviation from the $\mu = 1$ line at approximately 1 kG, and the magnetization curve peaks at approximately 2.1 kG, where $-4\pi M_I = 1.5$ kG. Beyond this value the slope reverses sign and approaches the H_a axis with a decreasing negative slope.

The higher-field points are seen to be scattered, and a discontinuous behavior (see Fig. 1) may be concealed in the noise. The solid line is the approximation to the data used in calculating the deviations from classical behavior in the self-excited case. The peak at 2.1 kG is at roughly one-half the lowest observed value of the first discontinuity in the magnitization curve for zero demagnetizing factor.[6] This is consistent with the notion that the field seen by a diamagnetic cylinder in a transverse field is twice the applied field at its surface. Although it should be pointed out that the field at the surface of the wire in the coil is certainly not as large as for an isolated transverse cylinder, the factor of two may be fortuitous and may be related to a size-dependent magnetization of the kind suggested by Bean.[12]

The results from step 5 are used in the same way to plot a magnetization curve (Fig. 5) which describes the history dependence of the remnant moment M_r. There is no measurable M_r up to $H_a \approx 500$ G, in good agreement with the value of 470 G for the first irreversible[6] field penetration. The increase is roughly linear from this point to 4.2 kG. After some oscillation, $-4\pi M_r$ saturates at a value of

1.5 kG. This is the same value as the maximum in the $-4\pi M_I$ curve. This is not unexpected, as it would seem that the defect structure would trap roughly the same field as it excludes. The value of H_a at the maximum is roughly twice the value of H_a at the maximum of the $-4\pi M_I$ curve. This is reasonable, since if field is excluded, there is no field to be trapped. At the value of H_a for the maximum in Fig. 4, the shielding currents can no longer increase, therefore field is permitted to leak in and consequently be trapped. The maximum occurs when H_a has been raised to twice the H_a for maximum shielding. The oscillation indicates that some flux jumping is occurring and, at least at lower fields, sizeable volumes of the coil are jumping at the same field. Again the solid curve is the approximation used to calculate H(z) in the self-excited case.

As a test of the assumption that M_r is constant over the coil and parallel to the z axis, Eq. (4) was used to calculate the z dependence of H_m; the calculated points are plotted on the continuous experimental curve in Fig. 6. The H_a was raised to 40 kG and reduced to zero. The agreement is quite good generally. There is some deviation at the ends, but this can be accounted for in terms of the variation of H_a in magnitude and direction over the coil volume.

Self-Excited Case

In a similar way the history dependence of $H_r(z)$, the remnant field in the bore of the magnet, was determined for the self-excited case; i.e., current flowing in the windings that results in $H_a(z)$. A typical $H_r(z)$ curve is exhibited in Fig. 7. The magnet current had been raised to 10A(H_a = 24.85 kG) and reduced to zero. The solid line is the measured $H_r(z)$ while the O are the calculated values. This curve was characterized by the magnitude of H_r at the three extrema as labeled: $H_r(0)$, the field at the center of the magnet; H_r-, the peak in the direction opposite to H_a; and H_r+, the peak in the direction of H_a. The measured behavior of these fields as a function of magnet current is given in Fig. 8 as the discrete points. The solid lines give the results of a calculation based on the uniform-field case, Fig. 5.

The calculation was performed by dividing the coil-winding volume axially and radially into 100 ring-shaped volumes of equal Δr and Δz. By means of an IBM 7090 program due to Garret,[13] based on a Gaussian integration approach, the absolute value of the field H_{ai} and its direction θ_i were calculated for the center of each square Δr by Δz for a given magnet current; Eq. (2) was integrated and summation (3) was performed. The appropriate $M_{ri}(H_a)$ was found from the data in Fig. 5 and its direction was taken as θ_i. The agreement between experimental data and the results of this calculation is good in view of the simplifying assumptions made. The discrepancy is of the order of 20 to 40%, which implies that though this kind of calculation may not be capable of great accuracy, it would be useful in estimating the magnitudes of these effects for a particular magnet.

The dependence of the self-field H(z) on magnet current (I) was investigated in a manner analogous to that for the uniform-field case, except that the current was not turned off between each measurement; i.e., step 4 was eliminated. Three cases were studied:

(a) virgin coil (cooled to 4.2°K with $I \equiv 0$),

(b) nonvirgin coil (I had been to 10.5 A),

(c) nonvirgin coil after reversal of current.

The resulting three curves for $|H(0)/I|$ vs $|I|$ are shown in Fig. 9. Curves b and c originate at $-\infty$ and $+\infty$, respectively, because of the remnant field $H_r(0)$. The curves are seen to coincide at approximately 3.5 kG (1.4 A), where the apparent $|H/I|$ is 2.560 kG/A. This should be compared with the value 2.485 kG/A, the value calculated on a $\mu = 1$ basis—shown as a horizontal line in Fig. 9. Beyond 1.4 A, $|H/I|$—though not constant—nevertheless behaves apparently in a history-dependent way, clearly making an asymptotic approach to the $\mu = 1$ line. This is expected from the breakdown of perfect diamagnetism in the way described by Figs. 1 and 4.

From the data of Fig. 4, the behavior of the virgin |H/I| curve was predicted in the same way as in the remnant-field case. The results of this calculation are shown as the solid line in Fig. 9. The agreement is seen to be perfect within experimental error above 1.5A. Below 0.5 A the solid curve is flat, corresponding to the measured perfect diamagnetism of the wire and the assumption that the field at the site of a particular volume of the wire is the same as the $\mu = 1$ case. Under these conditions one can show

$$\left|\frac{H(0)}{I}\right|_{\text{true}} = \left|\frac{H(0)}{}\right|_{\mu=1} G \tag{5}$$

for the perfect diamagnetic coil, where G is a geometry-dependent contstant factor, which for this case is 1.113. The failure of the experimental data to show this constant behavior below 0.5 A can be taken to indicate the breakdown of the assumptions under which G was calculated. The maximum observed value of H/I for the virgin case is 3.111 kG/A at 0.012 A.

Although the accuracy of the H(z) measurements reported here does not permit experimental verification of the behavior of the quantity $\Delta H/\Delta I$, a few comments based on the nature of the magnetization of Nb-Zr may be in order. Figure 1 reveals that following a jump, the material is almost perfectly diamagnetic for a small excursion in H_a. This implies that, for small changes in current, $\Delta H(0)/\Delta I$ does not approach the $\mu = 1$ value smoothly except in the limit as H throughout the winding volume approaches the resistive critical field. In a real magnet, however, the fields are not this high because the critical currents are so low that it is not practical to construct magnets that operate in this region. Further, any magnet has a field gradient through the winding volume, so that no matter what the central field may be there are always regions that are acting diamagnetically. The detailed calculation of the magnitude of this effect in a particular magnet is involved, and precise calculations would seem to be rather difficult and uncertain because they would be based on a magnetization curve whose discontinuities depend on position, amplitude, and such difficult-to-handle parameters as history, cold work, rate of rise of H_a, and shape. In the worst case, in which most of the wire had just "jumped" and therefore was acting strongly diamagnetic, $\Delta H(0)/\Delta I$ for this magnet according to Eq. (5) would be as high as 2.765 kG/A-11% higher than the asymptotic value. It is unlikely that fluctuations of this magnitude would occur at high fields, since the strong variation of H_a in the winding volume would certainly have a significant averaging effect. In this magnet, the strong scatter of the experimental points between 2 and 4 A suggests that strong variations in $\Delta H/\Delta I$ do occur.

In the three cases studied H(z) is, of course, not simply behaved, particularly at low fields. Below 1.4 A both the remnant field and the diamagnetic field must be considered as contributing to the central field. Above 1.4 A the diamagnetic effects appear to dominate and behave as a function of current in a manner consistent with Fig. 9. Figure 10 shows H(z) at I = 1.05 A for the virgin coil. The dashed curve is H(z) as calculated for $\mu = 1$; the dotted curve is as calculated by using Eq. (3) and performing the summation as in the remnant-field case. The agreement is excellent beyond 1 cm. It is correct in predicting better uniformity and a higher field in the center. Figure 11 shows H(z) for I = 0.257 A in the nonvirgin case. The dashed curve has the same significance as before. The contribution of the remnant field (Fig. 7) is clearly evident. The calculated curve takes account of both remnant field and induced field, thus:

$$H = H_a + H_{I,\,calc} + H_{r,\,calc} . \qquad (6)$$

As with all polarization effects, it is necessary to go to long magnet lengths to minimize H_m effects; i.e., $r_2/\ell << 1$. In fact, it is clear that $H_m \propto 1/\ell^2$ in such a case. At the other extreme, for a uniform H_a and perfect diamagnetism—with $r_2/r_1 >> 1$, $r_2 >> \ell$—we have $H_z = H_a\,[(2 - \ell/r_2)] \approx 2\,H_a$. In the self-excited case the result is not so simple, but it is clear that H_m will be an important contribution to the field in the bore of short magnets.

RELATED MEASUREMENTS

The critical current, I_c, of a short sample of the wire making up the coil was measured as a function of applied transverse magnetic field. The I_c is defined as the current at which the first measurable resistance appears. The measurement was made at 4.2°K in a manner equivalent to that reported by the author in an earlier paper.[14] The results are given in Fig. 12, and exhibit behavior typical of hard-drawn Nb-25% Zr alloy wire. The dashed line is the 2.532-kG/A line describing the maximum coil field, and the point at which the coil operates at its maximum current is marked (*). This operating point is clearly below the intersection of the dashed line and the short-sample curve. The most straightforward interpretation of the meaning of the intersection is, of course, that it represents the expected operating points of the magnet. It has been almost the universal experience that unless this point is well down on the steep part of the I_c-vs-H curve and near or below 20 A, it never coincides with the coil operating point. Coil critical currents for 0.025-cm-diam wire are invariably near 20 A, roughly independent of the I_c-vs-H curve and of the load line of the particular coil; the only qualification is that the coil have "many" layers.

It has been clearly shown that this so-called "20-ampere catastrophe" is not related to the statistical variation of the I_c-vs-H properties along the length of the wire. This was demonstrated by winding a long length (100 ft) of Nb-25% Zr wire in such a way that the wire was well decoupled magnetically, then measuring its I_c-vs-H curve. It exhibited the typical short-sample behavior. It was then wound tightly into a many-layer magnet, and the critical current was 25 A. It was then unwound and the sequence repeated with identical results.

The various explanations offered for this anomaly all relate to the nature of the magnetization of the superconductor. In general they are unsatisfying. Montgomery proposes that the diamagnetic shielding currents somehow subtract from the true critical current.[15] It is not clear, however, why the measured I_c-vs-H curves fail to automatically account for this. The objection also applied to Chandrasekhar and Hulm,[16] who extended this idea but failed to solve the problem in sufficient detail to give a meaningful criterion.

Another feature of the magnetization curve, which may imply uncertainties in coil critical currents, is the flux jump. The heat associated with the jump can easily be seen to be of sufficient magnitude to raise the temperature locally to a value in excess of the transition temperature of Nb-25% Zr. The sudden entry of flux in one part of the coil may induce jumps in other parts, resulting in an avalanche-like transition to the normal state. The details of this are very difficult to work out, as the description of this phenomenon would depend on a detailed knowledge of the magnetization curve as a function of current and time-rate-of-change of current, field, time-rate-of-change of field, size, orientation, and thermal coupling to the bath. In support of the usefulness of this approach is the empirical knowledge[17] that coating the superconductor with copper is effective in raising I_c of Nb-Zr magnets. The copper apparently acts as an eddy-current damping element and will act to reduce dH_a/dt, possibly decrease the thermal resistances to the bath, and provide a volume of material other than the superconductor in which to dissipate the heat. All these effects seem to be in such a direction as to reduce the probability that the superconductor would leave its metastable high-current-carrying state.

The inductance of the coil was measured as a function of an externally applied uniform field parallel to the axis. The measurement was made at 1 kc at 4.2°K. The maximum measuring current was 30 mA. The results are given in Fig. 13. The measured inductance of the coil in the superconducting state is 0.720 H at zero field; it rises linearly to 0.750 H at 60 kG, then increases rapidly to its 77°K value of 1.42 H at 75 kG. The calculated value for the $\mu = 1$ case is 1.46 H, in good agreement with the 77°K value. The reduction of the inductance of the coil when in the superconducting state is, of course, due to the apparent diamagnetism of the winding volume.

ACKNOWLEDGMENTS

The author wishes to express his gratitude to Richard Wolgast and Kenneth Solomon for their valuable assistance in taking the data. Honors are due Ernest Wellington and Donald Fong for their excellent mechanical work, and Thomas O'Halloran for acting as the coupling between the author and the IBM 7090. I also wish to thank Harley C. Hitchcock for supplying the magnetization curve, Fig. 1.

FOOTNOTES AND REFERENCES

* Work done under the auspices of the U. S. Atomic Energy Commission.

† Present address: NASA, Lewis Research Center, Cleveland, Ohio.

1. J. E. Kunzler, E. Buehler, F. S. L. Hsu, and J. H. Wernick, Phys. Rev. Letters 6, 39 (1961).
2. T. G. Berlincourt, R. R. Hake, and D. H. Leslie, Phys. Rev. Letters 6, 671 (1961).
3. J. E. Kunzler, in Proceedings of the 1961 International Conference on High Magnetic Fields (M.I.T. Press and John Wiley & Sons, Inc., New York, 1962), p. 574.
4. J. K. Hulm, M. J. Fraser, H. Riemersma, A. J. Venturino, and R. A. Wien, in Proceedings of the 1961 International Conference on High Magnetic Fields (M.I.T. Press and John Wiley & Sons, Inc., New York, 1962), p. 332.
5. R. C. Wolgast, H. P. Hernandez, P. R. Aron, H. C. Hitchcock, K. A. Solomon, Advan. Cryog. Eng. 8 (in press).
6. Harley C. Hitchcock (Lawrence Radiation Laboratory, Berkeley, California), private communication, 1963.
7. Y. B. Kim, C. F. Hempstead, and A. R. Strnad, Phys. Rev. Letters 9, 306 (1962).
8. A. A. Abrikosov, Soviet Phys. JETP (English Transl.) 5, 1174 (1957).
9. P. W. Anderson, Phys. Rev. Letters 9, 309 (1962).
10. R. F. K. Herzog and O. Tischler, Rev. Sci. Instr. 24, 1000 (1953).
11. D. B. Montgomery, Report of National Magnet Laboratory, AFOSR-1526, Massachusetts Institute of Technology, November 1961.
12. C. P. Bean, Phys. Rev. Letters 8, 250 (1962).
13. This program was supplied to the authors by Dr. C. E. Parker, Oak Ridge National Laboratory.

14. P. R. Aron and H. C. Hitchcock, J. Appl. Phys. 33, 2242 (1962).

15. D. B. Montgomery, Appl. Phys. Letters 1, 41 (1962).

16. B. S. Chandrasekhar and J. K. Hulm, Appl. Phys. Letters 2, 43 (1962).

17. R. C. Wolgast and P. R. Aron (in preparation).

FIGURE LEGENDS

Fig. 1. Magnetization vs H_a of Nb-25% Zr long cylinder in a field applied parallel to the long axis at 4.2°K. The field was swept at 300 Oe/sec.

Fig. 2. Diagram of magnet circuit and field-measuring apparatus.

Fig. 3. Diagram of coil subdivision.

Fig. 4. $-4\pi M_I$ vs H_a for uniform applied field.

Fig. 5. $4\pi M_r$ vs H_a for uniform applied field.

Fig. 6. $-H_r$ vs z for uniform applied field. The applied field had been to 93.5 kG. ○ calculated points; — measured.

Fig. 7. $-H_r$ vs z for the self-excited case. The current had been to 10.5 A. — measured; ○ calculated.

Fig. 8. H_r vs I for the self-excited case. ○ $H_r(0)$ measured; ΔH_r - measured; □ H_r + measured.

Fig. 9. $\left|\frac{H}{I}\right|$ vs I. ○ virgin coil as measured; □ nonvirgin coil as measured; △ nonvirgin coil after reversal of current; — calculated curve for virgin case.

Fig. 10. H vs z for 1.054 A in the virgin case. — measured; --- $\mu = 1$ calculation; •••• calculated from Eq. (3).

Fig. 11. H vs z for 0.257 A in the nonvirgin case. — measured; --- $\mu = 1$ calculation; •••• calculated from Eq. (6).

Fig. 12. I_c vs H_a for a short sample of the wire used in the magnet. ○ measured points; ---- 2.532 kG/A line; * maximum critical current of coil.

Fig. 13. Coil inductance (1 kc) vs applied uniform magnetic field. ○ measured points.

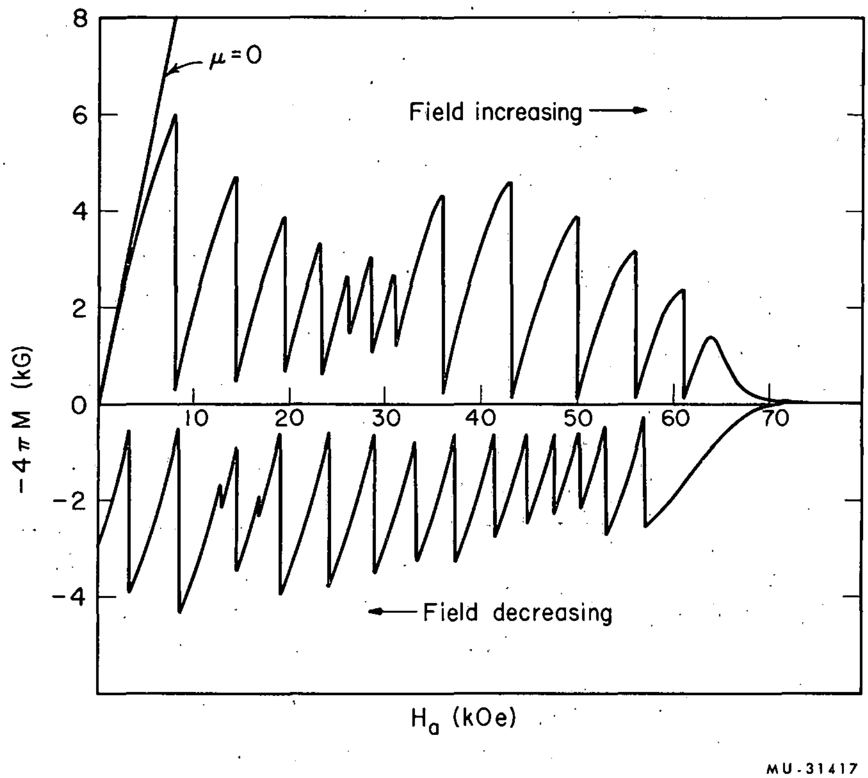
μ=0
Field increasing
Field decreasing
8
6
4
2
0
-2
-4
10
20
30
40
50
60
70
−4πM (kG)
Ha (kOe)
MU-31417

Fig. 1

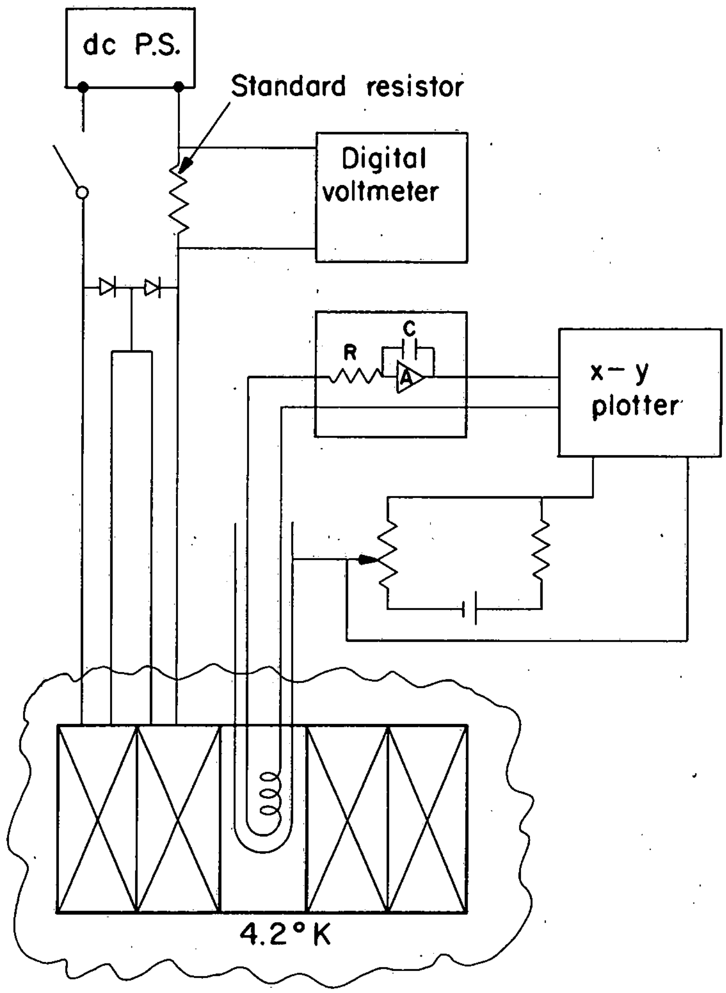
dc P.S.
Standard resistor
Digital voltmeter
R
C
A
x- y plotter
4.2°K
MU-31415

Fig. 2

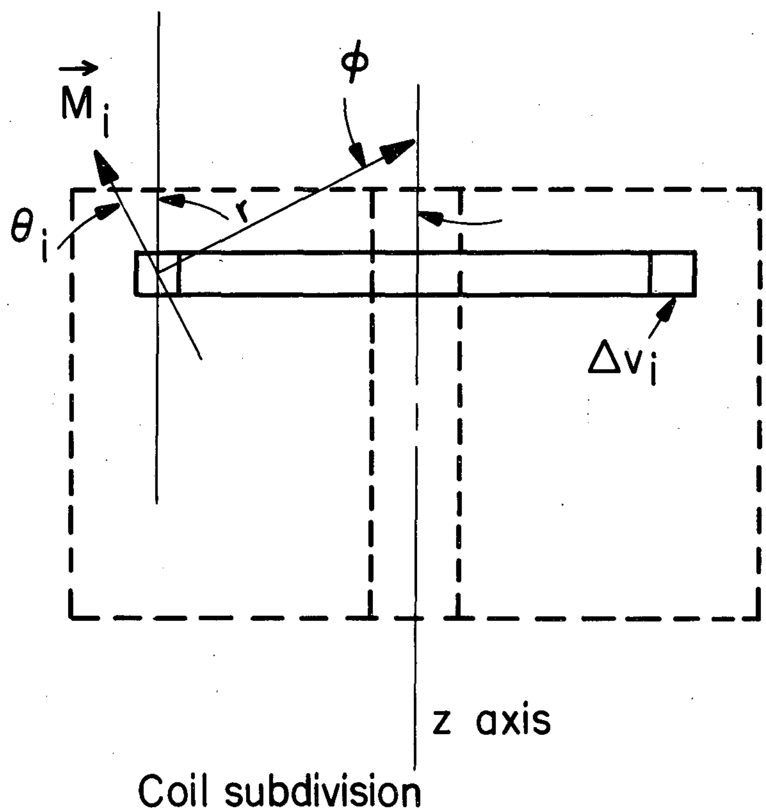

MU-31416

Fig. 3

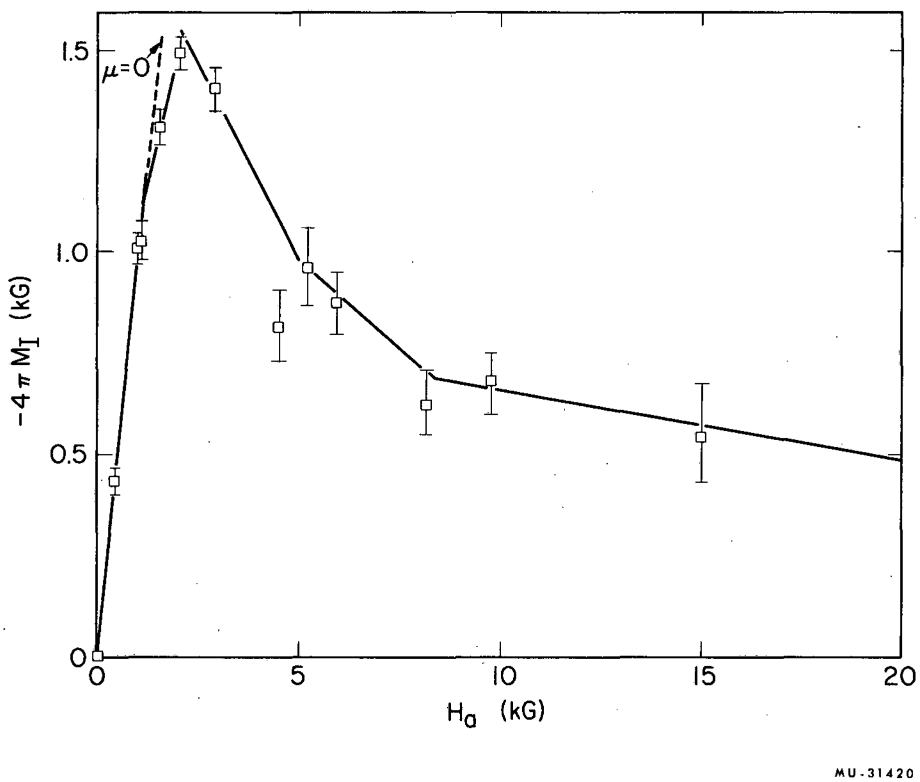

Fig. 4

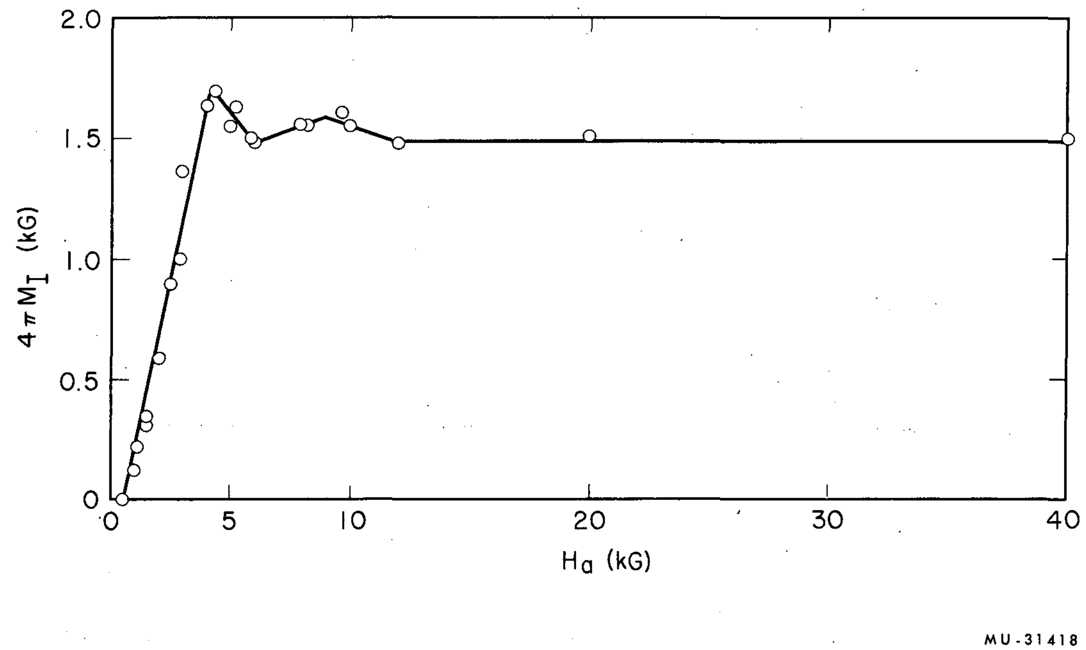

Fig. 5

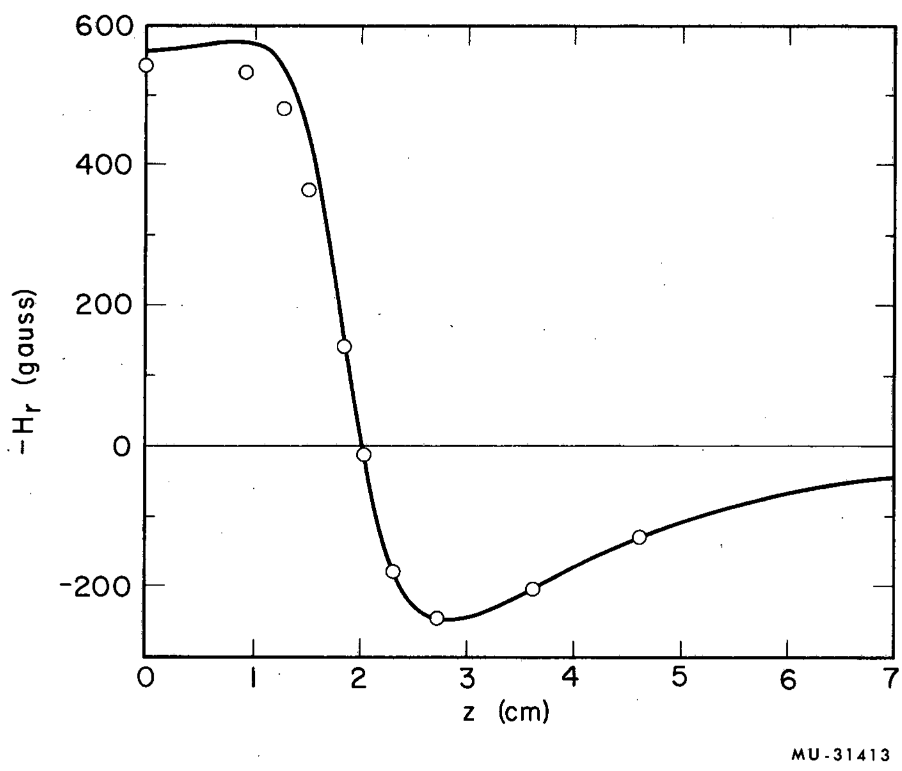

Fig. 6

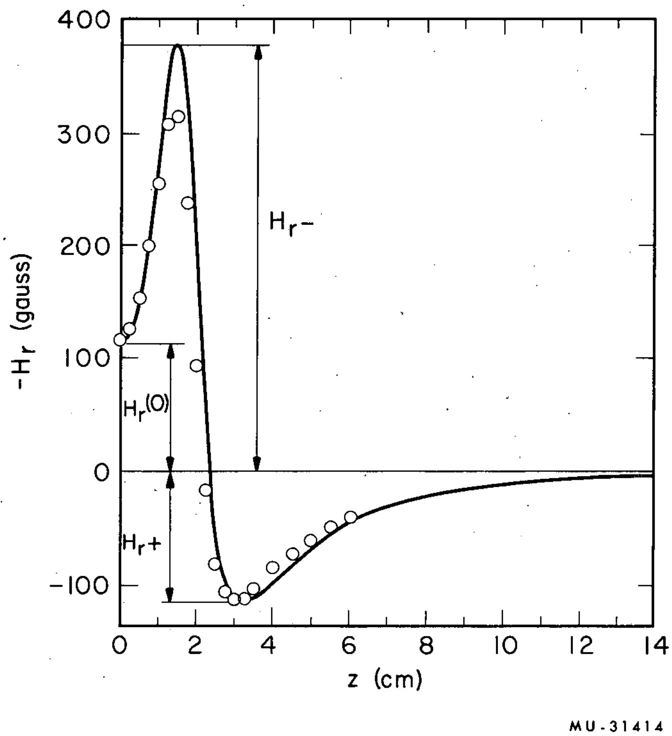
400
300
200
100
0
-100
$-H_r$ (gauss)
H_r-
$H_r(0)$
H_r+
0
2
4
6
8
10
12
14
z (cm)
MU-31414

Fig. 7

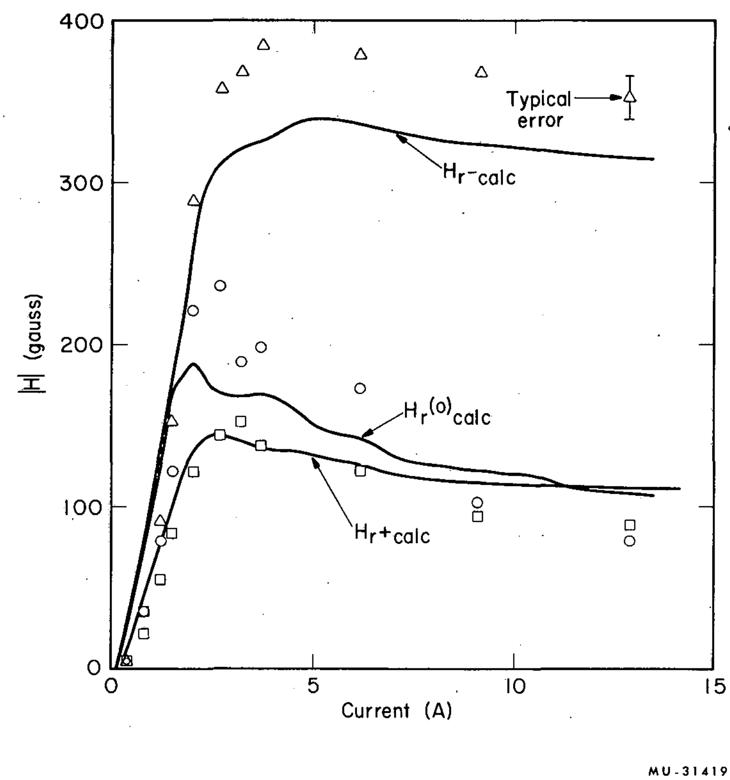

400
300
200
100
0
|H| (gauss)
0
5
10
15
Current (A)
Typical error
H_r-calc
$H_r(o)$calc
H_r+calc
MU-31419

Fig. 8

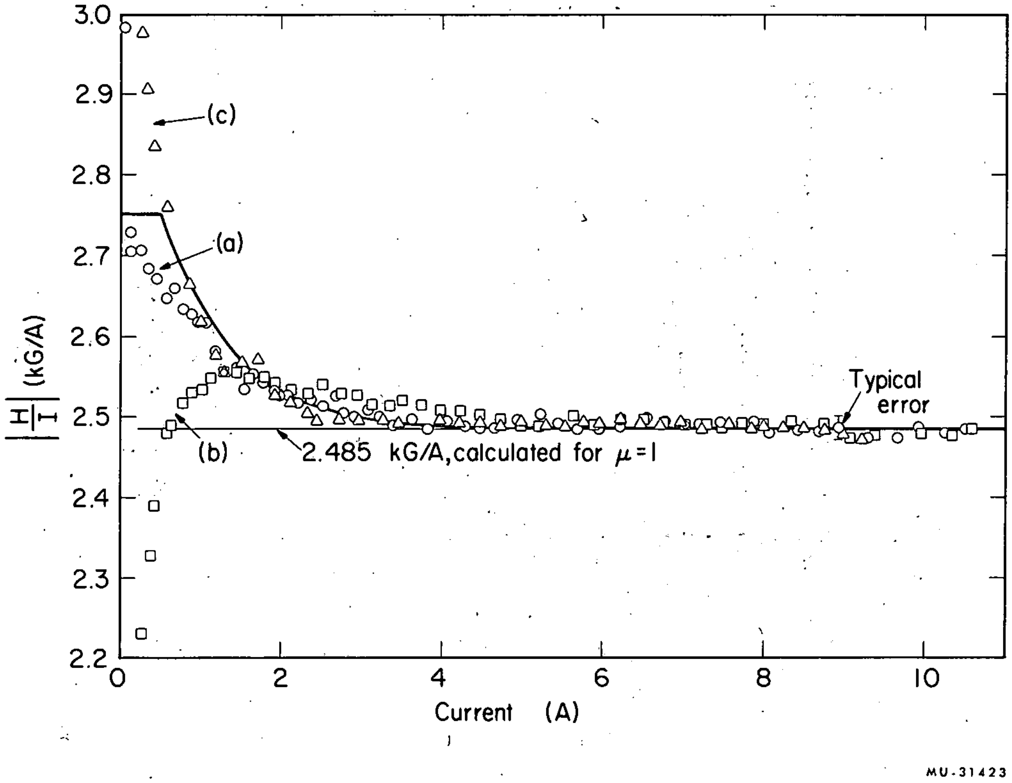
3.0
2.9
2.8
2.7
2.6
2.5
2.4
2.3
2.2
|H/I| (kG/A)
(c)
(a)
(b)
2.485 kG/A, calculated for μ=1
Typical
error
0
2
4
6
8
10
Current (A)
MU-31423

Fig. 9

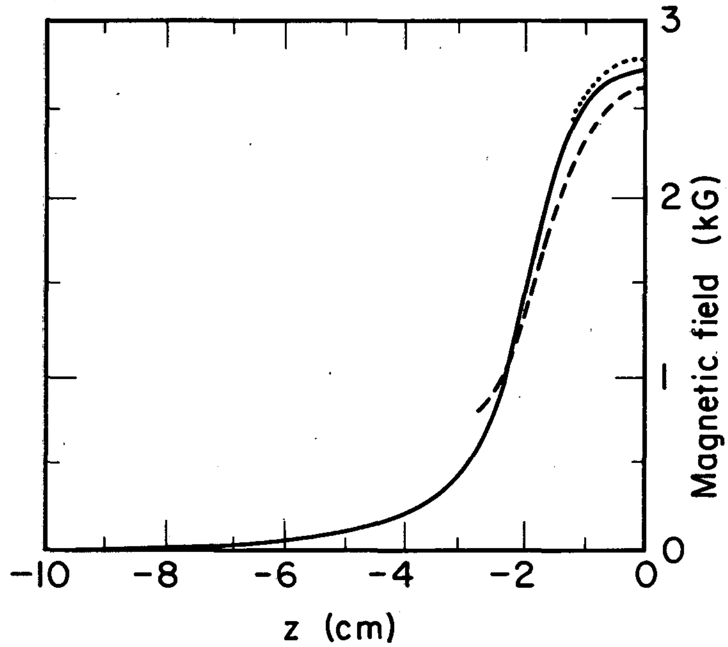

MU-31411

Fig. 10

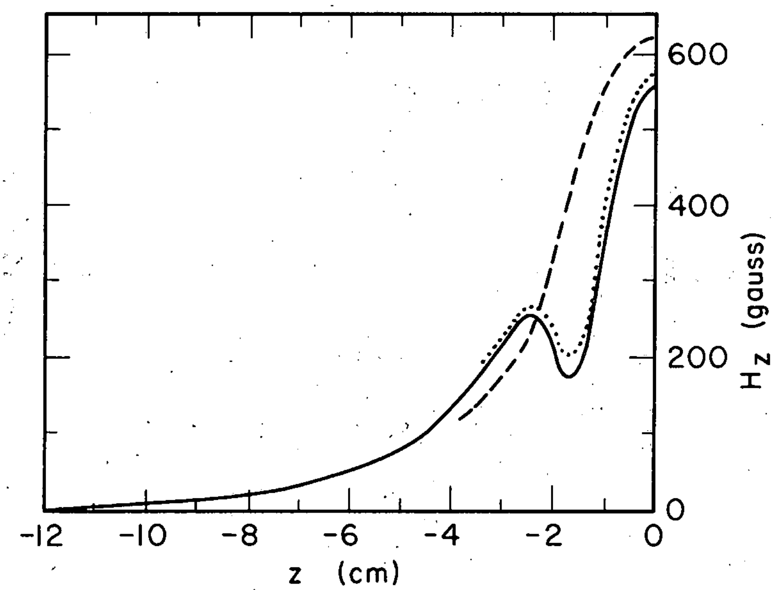

MU-31412

Fig. 11

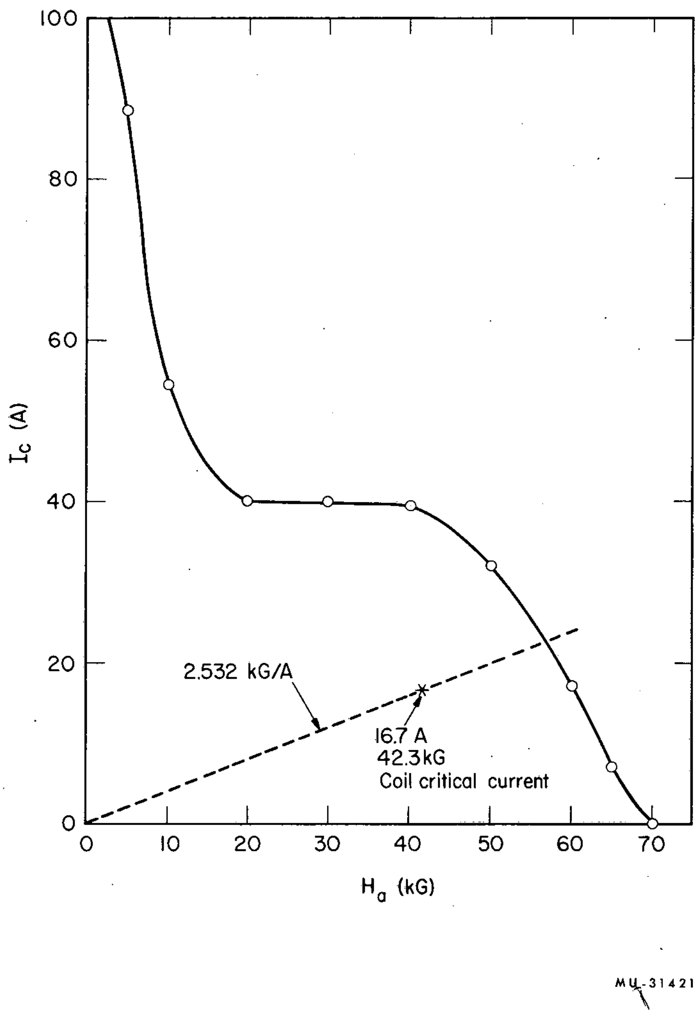
100
80
60
40
20
0
I_c (A)
0
10
20
30
40
50
60
70
H_a (kG)
2.532 kG/A
16.7 A
42.3kG
Coil critical current
MU-31421

Fig. 12

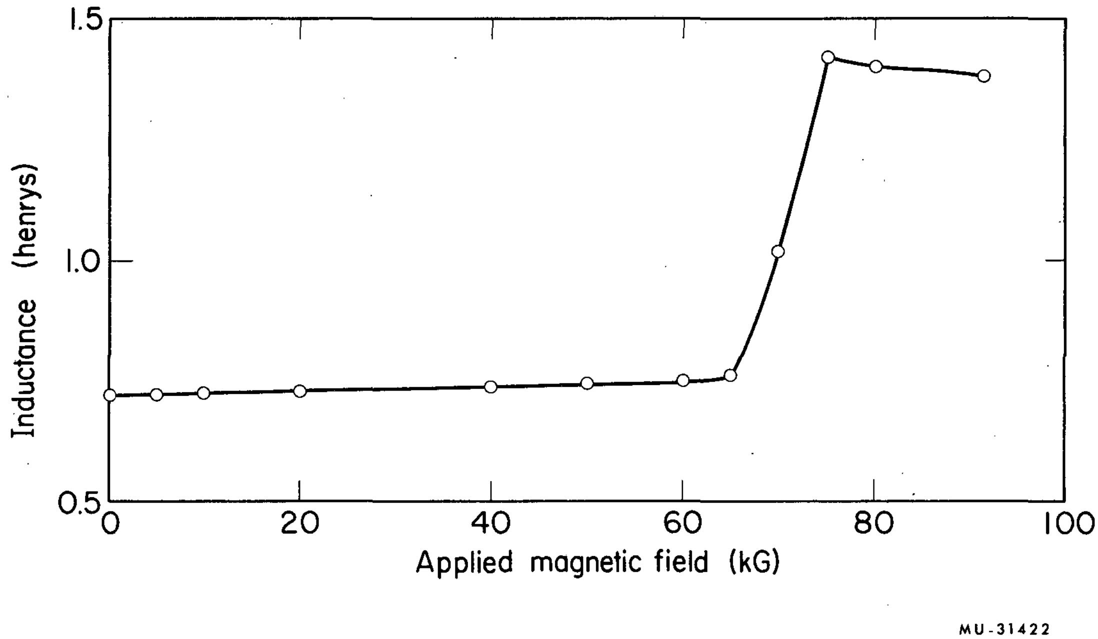
1.5
1.0
0.5
Inductance (henrys)
0
20
40
60
80
100
Applied magnetic field (kG)
MU-31422

Fig. 13